

PCCP

Accepted Manuscript



This is an *Accepted Manuscript*, which has been through the Royal Society of Chemistry peer review process and has been accepted for publication.

Accepted Manuscripts are published online shortly after acceptance, before technical editing, formatting and proof reading. Using this free service, authors can make their results available to the community, in citable form, before we publish the edited article. We will replace this *Accepted Manuscript* with the edited and formatted *Advance Article* as soon as it is available.

You can find more information about *Accepted Manuscripts* in the [Information for Authors](#).

Please note that technical editing may introduce minor changes to the text and/or graphics, which may alter content. The journal's standard [Terms & Conditions](#) and the [Ethical guidelines](#) still apply. In no event shall the Royal Society of Chemistry be held responsible for any errors or omissions in this *Accepted Manuscript* or any consequences arising from the use of any information it contains.

Unconventional $\text{CH}^{\delta+} \dots \text{N}$ Hydrogen Bonding Interactions in the Stepwise Solvation of the Naphthalene Radical Cation by Hydrogen Cyanide and Acetonitrile Molecules

Sean P. Platt, Isaac K. Attah and M. S. El-Shall*

Department of Chemistry, Virginia Commonwealth University
Richmond, VA 23284-2006

Rifaat Hilal^{a,b}, Shaaban A. Elroby^{a,c} and Saadullah G. Aziz^a

^{a)} Department of Chemistry, Faculty of Science, King Abdulaziz University
Jeddah 21589, Saudi Arabia

^{b)} Department of Chemistry, Faculty of Science, Cairo University, Giza, Egypt

^{c)} Department of Chemistry, Faculty of Science, Beni-Seif University, Beni-Suef, Egypt

Abstract

Equilibrium thermochemical measurements using the mass-selected ion mobility (MSIM) technique have been utilized to investigate the binding energies and entropy changes of the stepwise association of hydrogen cyanide (HCN) and acetonitrile (CH_3CN) molecules with the naphthalene radical cation ($\text{C}_{10}\text{H}_8^{\bullet+}$) in the gas phase forming the $\text{C}_{10}\text{H}_8^{\bullet+}(\text{HCN})_n$ and $\text{C}_{10}\text{H}_8^{\bullet+}(\text{CH}_3\text{CN})_n$ clusters with $n = 1-3$ and $1-5$, respectively. The lowest energy structures of the $\text{C}_{10}\text{H}_8^{\bullet+}(\text{HCN})_n$ and $\text{C}_{10}\text{H}_8^{\bullet+}(\text{CH}_3\text{CN})_n$ clusters for $n = 1-2$ have been calculated using the M062X and ω 97XD methods within the 6-311+G** basis set, and for $n = 1-6$ using the B3LYP method within the 6-311++G** basis set. In both systems, the initial interaction occurs through unconventional $\text{CH}^{\delta+} \dots \text{N}$ ionic hydrogen bonds between the hydrogen atoms of the naphthalene cation and the lone pair of electrons on the N atom of the HCN or the CH_3CN molecule. The binding energy of CH_3CN to the naphthalene cation (11 kcal/mol) is larger than that of HCN (7 kcal/mol) due to a stronger ion-dipole interaction resulting from the large dipole moment of CH_3CN (3.9 D). On the other hand, HCN can form both unconventional hydrogen bonds with the hydrogen atoms of the naphthalene cation ($\text{CH}^{\delta+} \dots \text{NCH}$), and conventional linear hydrogen bonding chains involving $\text{HCN} \dots \text{HCN}$ interactions among the associated HCN molecules. HCN molecules tend to form “externally solvated” structures with the naphthalene cation where the naphthalene ion is hydrogen bonded to the exterior of an $\text{HCN} \dots \text{HCN}$ chain. For the $\text{C}_{10}\text{H}_8^{\bullet+}(\text{CH}_3\text{CN})_n$ clusters, “internally solvated” structures are favored where the acetonitrile molecules are directly interacting with the naphthalene cation through $\text{CH}^{\delta+} \dots \text{N}$ unconventional ionic hydrogen bonds. In both the $\text{C}_{10}\text{H}_8^{\bullet+}(\text{HCN})_n$ and $\text{C}_{10}\text{H}_8^{\bullet+}(\text{CH}_3\text{CN})_n$ clusters, the sequential binding energy decreases stepwise to about 6-7 kcal/mol by three HCN or CH_3CN molecules, approaching the macroscopic enthalpy of vaporization of liquid HCN (6.0 kcal/mol).

Keywords: Ion-neutral complexes; Naphthalene radical cation; Unconventional ionic hydrogen bonds; Binding energies of HCN and CH_3CN to organic ions; Solvation of organic cations with hydrogen cyanide and acetonitrile.

1. Introduction

Ionic hydrogen bonds (IHBs), involve hydrogen bonding between radical ions or protonated molecules and neutral polar molecules such as water, methanol, ammonia, and hydrogen cyanide.¹ IHBs have bond strengths higher than the typical conventional hydrogen bond in neutral systems and could reach up to 35 kcal/mol, nearly a third of the strength of covalent bonds.¹ These strong interactions are critical in many fields such as ion induced nucleation, ion solvation, radiation chemistry, electrochemistry, and self-assembly in supramolecular chemistry.¹⁻⁵ IHBs are also important in biological systems including peptides, protein folding, proton transport, enzyme active centers, and molecular recognition.⁶ Organic ions can form hydrogen bonds with solvents in nature, for example, in icy grains doped with aromatic and polycyclic aromatic hydrocarbons (PAHs) that are subjected to ionizing radiation in interstellar dust grains.⁷⁻¹⁰

Unconventional carbon-based IHBs are formed when the hydrogen donors are ionized hydrocarbons containing CH groups and the hydrogen acceptors are electron lone pairs on hetero atoms such as O and N, or π elections in olefin double bonds and aromatic conjugated systems.¹ For example, carbon-based $\text{CH}^{\delta+} \cdots \text{O}$ IHBs appear in the hydration of ionized aromatics such as benzene (C_6H_6^+), cyclic C_3H_3^+ , cyclobutadiene (C_4H_4^+), phenylacetylene (C_8H_6^+), and naphthalene ($\text{C}_{10}\text{H}_8^+$).¹¹⁻¹⁶ Organic ions can also interact with water molecules by stronger conventional hydrogen bonds, such as in protonated pyridine or protonated pyrimidine where the $\text{NH}^+ \cdots \text{O}$ hydrogen bonds can be formed.^{1,17,18}

In addition to water, other polar molecules containing lone pairs of electrons such as hydrogen cyanide and acetonitrile can participate in $\text{CH}^{\delta+} \cdots \text{N}$ IHBs with the ring hydrogen atoms ($\text{CH}^{\delta+}$) of ionized aromatics. Specifically, HCN has received considerable attention because of its role in atmospheric chemistry as a result of its release by biomass burning,¹⁹ and is also one of the main interstellar/nebula molecules.²⁰ HCN can be produced in space from the reactions of ammonia and methane, and HCN polymers have been shown to exist in meteorites, comets, planets, moons, and in circumstellar envelopes.²¹⁻²³ HCN is also postulated to be the source of nitrogen in the formation of nitrogen-containing polycyclic aromatic hydrocarbons (NPAHs) which could lead to the formation of biologically significant molecules such as DNA, RNA, and

proteins in space.²¹ A fundamental understanding of the reactions and structures of nitrogen-containing species in space may provide insights into the origin or origins of life.²¹⁻²⁵

We recently studied the stepwise association of multiple HCN molecules with the benzene, substituted benzene, phenylacetylene, pyridine and pyrimidine radical cations.²⁶⁻²⁹ In the benzene⁺⁺(HCN)_n clusters, HCN molecules are bonded to the benzene hydrogens by -CH^{δ+}---N hydrogen bonds, but linear hydrogen bonded HCN---HCN---HCN chains are also formed with further HCN molecules.^{26,27} In the phenylacetylene⁺⁺(HCN)_n clusters, the dominant interaction is hydrogen bonding between the C-H acetylenic hydrogen and the nitrogen atom of the first HCN molecule.²⁸ Subsequent HCN molecules form linear hydrogen bonded chains extended from the phenylacetylene radical cation [phenylacetylene⁺⁺(NCH---NCH---)].²⁸ Such chains were proposed previously in protonated (HCN)_nH⁺ clusters (HCN---(HCN---H⁺---NCH)---NCH) where binding enthalpies indicated completion of solvent shells by two (first shell) or four (second shell) HCN molecules about the proton.^{1,30} The pyridine and pyrimidine radical cations form unconventional carbon-based ionic hydrogen bonds with HCN molecules where bifurcated structures involving multiple hydrogen bonding sites with the ring hydrogen atoms are formed. Protonated pyridine forms a stronger ionic hydrogen bond with HCN (NH⁺...NCH) which can be extended to a linear chain with the clustering of additional HCN molecules (NH⁺...NCH ···NCH...NCH) leading to a rapid decrease in the bond strength as the length of the chain increases.²⁹

Here, we present the first experimental and computational study of the stepwise association of HCN and CH₃CN molecules with the naphthalene radical cation (C₁₀H₈⁺) in the gas phase using the mass-selected ion mobility (MSIM) technique.^{11-18,29} The thermochemical ion-molecule equilibrium measurements, when conducted at different temperatures, yield the enthalpy and entropy changes of the stepwise association of solvent molecules with the organic ions. In the current systems, both HCN and CH₃CN (dipole moments = 2.98 and 3.91 Debye, respectively)³¹ contain N lone-pairs which can serve as hydrogen acceptors to the CH^{δ+} sites of the naphthalene radical cation. However, unlike HCN which can serve both as a hydrogen donor and as a lone-pair hydrogen acceptor, CH₃CN can't form linear H-bonding chains and favorable interactions may thus

occur with other $\text{CH}^{\delta+}$ sites of the naphthalene cation instead of sequential attachment to the CH_3CN molecules. To understand the nature of these interactions, we provide DFT calculations of the low energy structures of the naphthalene $^{*+}(\text{HCN})_n$ and naphthalene $^{*+}(\text{CH}_3\text{CN})_n$ clusters with $n = 1-6$. The combination of the experimental and computational results provides new insights into the factors that determine the energetics and structures of the naphthalene radical cation associated with HCN and CH_3CN molecules as model systems for the solvation of PAH ions within N-containing molecular clusters.

2. Methods

The experiments were performed using the VCU mass-selected ion mobility spectrometer. The details of the instrument can be found in several publications and only a brief description of the experimental procedure is given here.^{12,14,29} **Figure S1** (Supporting Information) illustrates the essential components of the ion mobility system. In the experiments, the naphthalene molecular ions ($\text{C}_{10}\text{H}_8^{*+}$) are formed by electron impact ionization using electron energy of 60-70 eV following the supersonic expansion of 40 psi (≈ 2500 Torr) of ultra-high pure helium seeded with about 1-2% of naphthalene vapor through a pulsed supersonic nozzle (500 μm) to the source vacuum chamber maintained at a background pressure of 10^{-7} Torr. $\text{C}_{10}\text{H}_8^{*+}$ ions are mass-selected by the first quadrupole mass-filter and injected in (30-50 μs pulses) into the drift cell which contains a mixture of HCN or CH_3CN vapor and a helium buffer gas. Flow controllers (MKS # 1479A) are used to maintain a constant pressure inside the drift cell within ± 1 mTorr. The temperature of the drift cell can be controlled to better than $\pm 1\text{K}$ using four temperature controllers. Liquid nitrogen flowing through solenoid valves is used to cool down the drift cell. The reaction products can be identified by scanning a second quadrupole mass filter located coaxially after the drift cell. The arrival time distributions (ATDs) are collected by monitoring the intensity of each ion as a function of time. The reaction time can be varied by varying the drift voltage. The injection energies used in the experiments (12–14 eV, laboratory frame) are slightly above the minimum energies required to introduce the naphthalene ions into the cell against the HCN/He or $\text{CH}_3\text{CN}/\text{He}$ outflow from the entrance orifice. Most of the ion thermalization occurs

outside the cell entrance by collisions with the HCN or CH₃CN molecules escaping from the cell entrance orifice. At a cell pressure of 0.2 Torr, the number of collisions that the C₁₀H₈⁺ encounters with the neutral molecules within the 1.5 millisecond residence time inside the cell is about 10⁴ collisions, which is sufficient to ensure efficient thermalization of the C₁₀H₈⁺ ions.

HCN is prepared by adding 8 g of sodium cyanide (NaCN) (Sigma-Aldrich, 97%) into a 500 ml stainless steel bubbler which is then placed in liquid nitrogen and evacuated followed by the addition of 4 ml of pure sulfuric acid (H₂SO₄) (Aldrich, 99.999%) through a stainless steel tube extension of the inlet valve of the bubbler. Following the reaction of sulfuric acid with the sodium cyanide salt inside the bubbler, HCN gas evolves and the bubbler is allowed to warm up to room temperature. The pressure in the HCN line is monitored by a Baratron pressure gauge (MKS-626A13TBD).

The equilibrium reactions are represented by equation (1)



where R = H or CH₃ for HCN or CH₃CN, respectively. The establishment of equilibrium is verified when: (1) a constant ratio of the integrated intensity of the product to the reactant ions is maintained over the residence time of the ions at constant pressure and temperature, and (2) the ATDs of the reactant and product ions are identical indicating equal residence times. When the equilibrium conditions are well-established, the equilibrium constant, K_{eq}, can be measured using equation (2):

$$K_{eq} = \frac{[\text{C}_{10}\text{H}_8^+(\text{RCN})_n]}{[\text{C}_{10}\text{H}_8^+(\text{RCN})_{n-1}][\text{RCN}]} = \frac{I[\text{C}_{10}\text{H}_8^+(\text{RCN})_n]}{I[\text{C}_{10}\text{H}_8^+(\text{RCN})_{n-1}] \cdot P_{\text{RCN}}} \quad (2)$$

Where $I[\text{C}_{10}\text{H}_8^+(\text{RCN})_{n-1}]$, $I[\text{C}_{10}\text{H}_8^+(\text{RCN})_n]$ are the integrated intensities of the ATDs of the reactant and product ions, respectively and P_{RCN} is the partial pressure of HCN or CH₃CN in atmosphere inside the drift cell. The equilibrium constant, K_{eq}, is measured at different temperatures and from a van't-Hoff plot, ΔH° and ΔS° values are obtained from the slope and intercept, respectively. The measured values are duplicated at least three

times and the average values are reported in Tables 1 and 2 with the corresponding uncertainties.

Density Functional Theory (DFT) calculations of the lowest energy structures for the various isomers of the cluster ions $C_{10}H_8^{+}(HCN)_n$ and $C_{10}H_8^{+}(CH_3CN)_n$ with $n = 1-2$ were performed using the M062X³² and ω 97XD³³ methods within the 6-311+G** basis set³⁴ of the Gaussian 09 program suite.³⁵ For larger clusters with $n = 3-6$, B3LYP method was used with the 6-311++G** basis set. Vibrational frequency calculations were also performed for all the optimized geometries at the same level of theory in order to obtain zero point vibrational energy (ZPVE) and also to verify the absence of any imaginary frequencies.³⁵

3. Results and Discussion

3.1. Association of HCN Molecules with the Naphthalene Radical Cation

Figure 1-a displays the mass spectrum obtained following the injection of the mass-selected $C_8H_{10}^{+}$ ion (m/z 128) into the drift cell containing 0.83 Torr He at 301 K. It is clear that no dissociation products are observed consistent with the low injection energy used (13.8 eV, lab). A small peak is observed at m/z 146 which corresponds to the $C_8H_{10}^{+}(H_2O)$ ion (labeled Naph⁺(W) in Fig. 1-a) due to the presence trace amount of water vapor in the drift cell. In the presence of 0.2 Torr HCN vapor in the drift cell at 273 K, the first two association products $C_8H_{10}^{+}(HCN)_n$ with $n = 1$ and 2 are observed as shown in Fig. 1-b. In addition, a small peak appears at m/z 100 assigned to the $H_3O^{+}(HCN)_3$ cluster ion formed by the association of three HCN molecules with the hydronium ion. This cluster ion exhibits enhanced intensity due to the formation of a stable solvent shell structure involving three IHBs from the hydronium ion to the nitrogen atoms of the three HCN molecules. As the temperature decreases the major cluster series $C_8H_{10}^{+}(HCN)_n$ shows a significant increase in intensity with a systematic shift towards larger n as shown in Figs 1-c 1-d and 1-e. At 177 K (the lowest achievable temperature before the condensation of HCN), the naphthalene ion disappears and the cluster population becomes dominated by the $C_8H_{10}^{+}(HCN)_n$ series with $n = 1-4$ as shown in Fig. 1-e.

The equilibrium constants for the stepwise association of HCN with the $C_8H_{10}^{*\dagger}$ ion (Reaction 1) measured at different temperatures yield the van't Hoff plots shown in Figure 2. From the slopes and intercepts of the van't Hoff plots, ΔH° and ΔS° values for the formation of the $C_8H_{10}^{*\dagger}(HCN)_n$ clusters are calculated as listed in **Table 1**.

The measured thermochemical values shown in **Table 1** indicate that the binding energies of the first three HCN molecules are nearly similar as $6-7 \pm 1$ kcal/mol. This suggests the presence of multiple binding sites with comparable energies for the HCN molecules to attach to the $C_8H_{10}^{*\dagger}$ ion. This interaction could involve C-H $^{\delta+}$...N unconventional hydrogen bonding where the naphthalene cation acts as the proton donor to the lone pair of electrons on the nitrogen atom of the HCN molecule. Additional HCN molecules could be attached to different C-H $^{\delta+}$ sites of the naphthalene cation or could form linear H-bonding chains by the attachment to the first HCN molecule associated with the naphthalene cation.

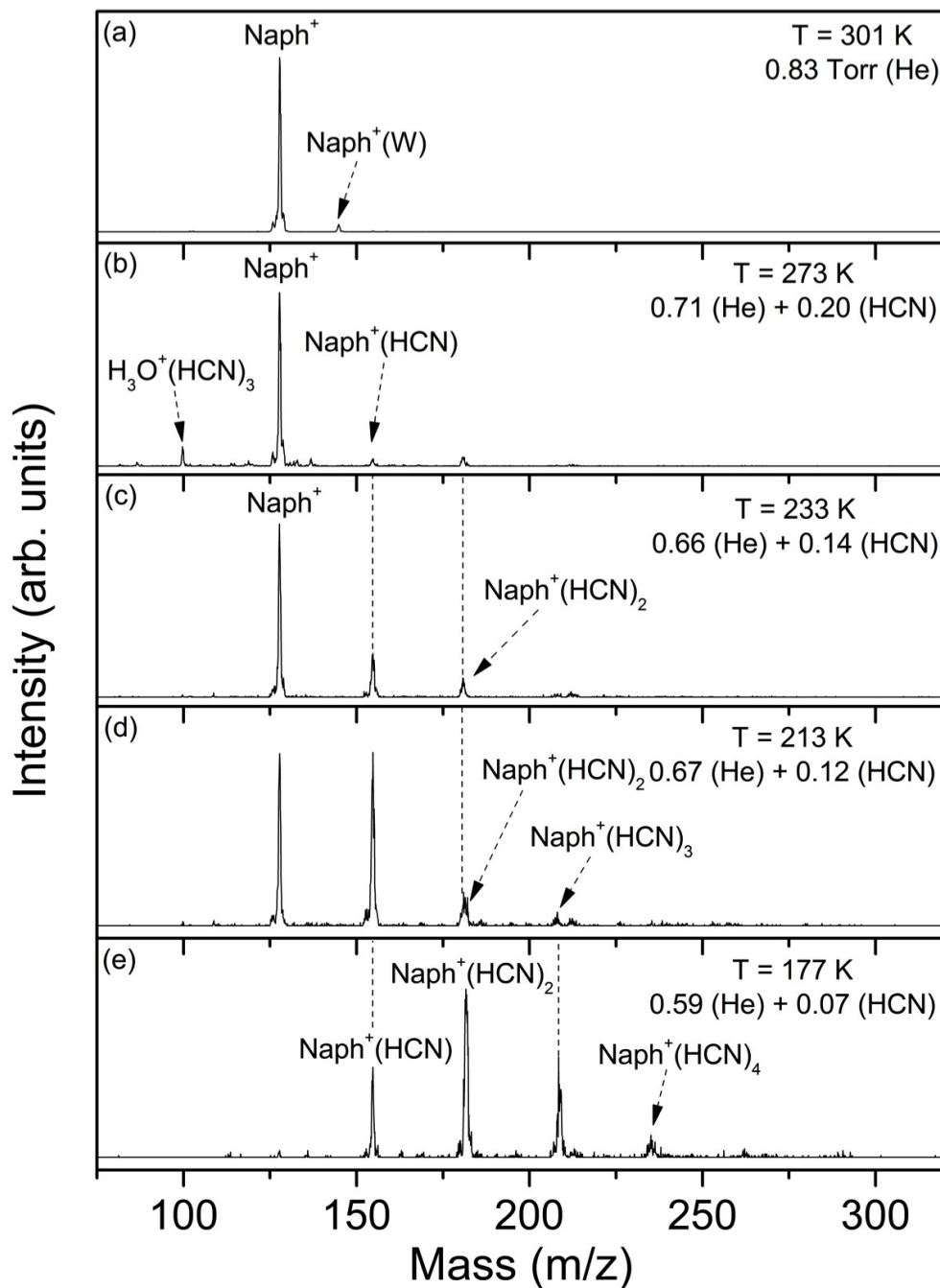


Figure 1. Mass spectra resulting from the injection of naphthalene radical cation ($\text{C}_{10}\text{H}_8^+$, Naph^+) into helium gas (a) or a helium-HCN vapor mixture (b-e) at different pressures and decreasing temperatures as indicated.

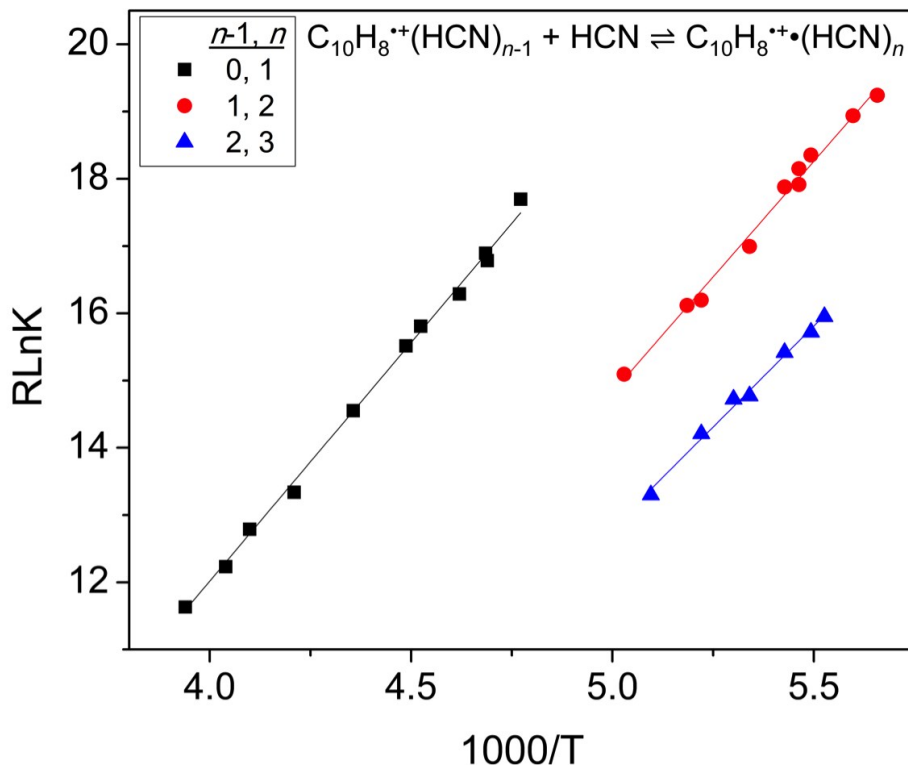


Figure 2. van't Hoff plot for resulting from the injection of naphthalene ($C_{10}H_8^+$) into HCN-He gas mixtures.

3.2 Association of CH_3CN with the Naphthalene Radical Cation

Figure 3 displays the mass spectra obtained upon the injection of the $C_8H_{10}^{\bullet+}$ ion into the drift cell in pure He and in the presence of 0.25 – 0.17 Torr CH_3CN vapor in He at different temperatures. At 301 K, most of the naphthalene ions are incorporated into the $C_8H_{10}^{\bullet+}(CH_3CN)_n$ clusters with $n = 1$ and 2 as shown in Fig. 3-b. The comparison with HCN at 273 K (Fig. 1-b) indicates that the binding of CH_3CN to the naphthalene cation is significantly stronger than that of HCN. This is clearly confirmed by the observation of the $C_8H_{10}^{\bullet+}(CH_3CN)_n$ clusters with $n = 1-3$ at 301 K as shown in Fig. 3-b while the $C_8H_{10}^{\bullet+}(HCN)_n$ clusters with $n = 1-2$ are only weakly observed at 273 K (Fig. 1-b). Interestingly, at the lowest temperature used (212 K), the $C_8H_{10}^{\bullet+}(CH_3CN)_n$ clusters

with $n = 2-5$ are the most prominent ions observed as shown in Fig. 3-d. Other ions observed include the $\text{H}_3\text{O}^+(\text{CH}_3\text{CN})_3$ cluster (m/z 142) which appears at 301 K and 244 K as shown in Figs 3-b and 3-c. This ion represents the first solvent shell of three acetonitrile molecules around the hydronium ion.³⁶ Interestingly at 212 K, the $\text{H}_3\text{O}^+(\text{CH}_3\text{CN})_3$ ion nearly disappears and the $\text{H}_5\text{O}_2^+(\text{CH}_3\text{CN})_4$ cluster (m/z 201) appears indicating the formation of a protonated water dimer core $(\text{H}_5\text{O}_2)^+$ solvated by four acetonitrile molecules through four conventional O-H δ^+ ...N IHBs.³⁷ It should be noted that acetonitrile liquid usually contains a trace amount of water which is very difficult to remove due to the strong interaction between water and acetonitrile in the liquid phase.³⁸ The van't Hoff plots of the first five CH_3CN additions onto the naphthalene cation are shown in Figure 4, and the resulting ΔH° and ΔS° are listed in **Table 1**.

Table 1. Measured thermochemistry ($-\Delta H^\circ_{n-1,n}$ and $-\Delta S^\circ_{n-1,n}$) of the formation of $\text{C}_8\text{H}_{10}^{*\dagger}(\text{HCN})_n$ and $\text{C}_8\text{H}_{10}^{*\dagger}(\text{CH}_3\text{CN})_n$ clusters.

n	HCN		Acetonitrile	
	$-\Delta H^\circ$	$-\Delta S^\circ$	$-\Delta H^\circ$	$-\Delta S^\circ$
1	7.1	16.4	11.3	20.9
2	6.6	18.0	9.2	17.3
3	6.0	17.2	7.2	15.0
4	-	-	8.0	23.2
5	-	-	7.7	22.1

(a) $\Delta H^\circ_{n-1,n}$ units are kcal/mol. (b) $\Delta S^\circ_{n-1,n}$ units are cal/mol.K, estimated errors: $\Delta H^\circ \pm 1$, $\Delta S^\circ \pm 2.0$.

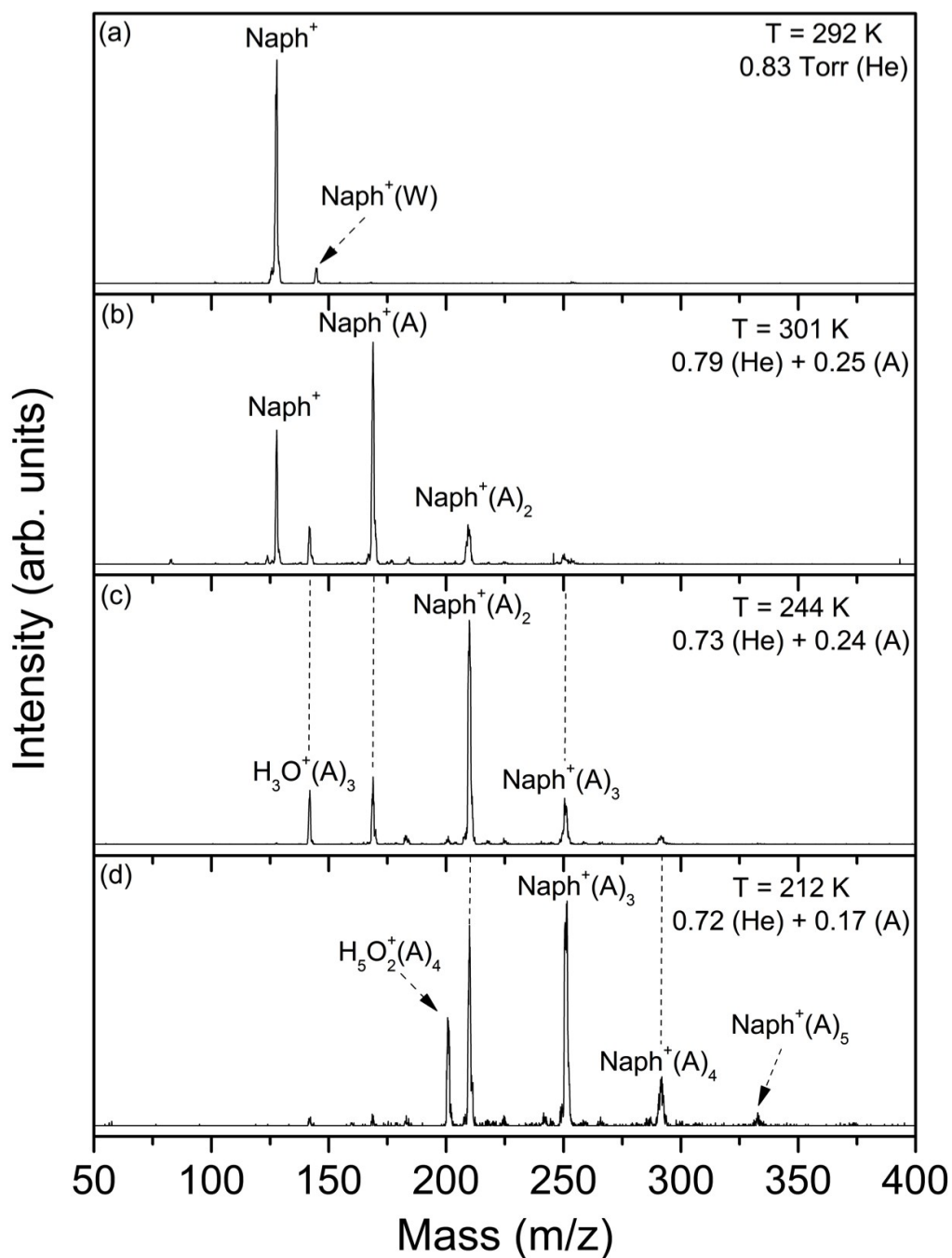


Figure 3. Mass spectra resulting from the injection of naphthalene radical cation ($\text{C}_{10}\text{H}_8^+$, Naph^+) into helium gas (a) or a helium-acetonitrile (CH_3CN , A) vapor mixture (b-d) at different pressures and decreasing temperatures as indicated.

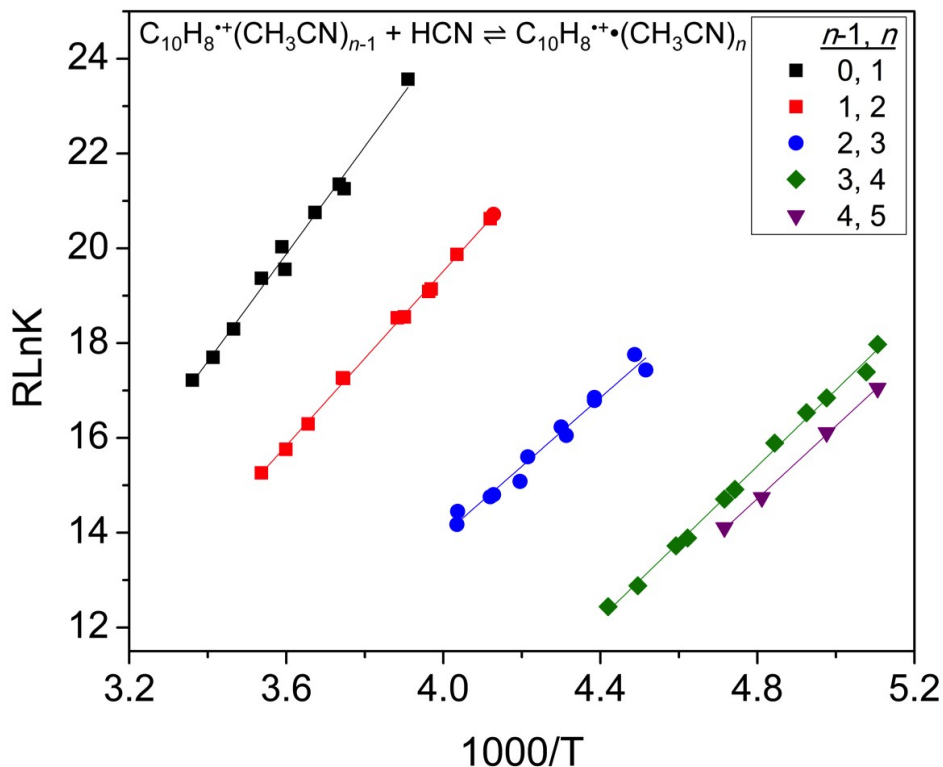


Figure 4. van't Hoff plot for resulting from the injection of naphthalene ($C_{10}H_8^+$) into acetonitrile (CH_3CN)-He gas mixtures.

3.3 Structures of the Naphthalene $^{++}(HCN)_n$ Clusters

To gain insight into the roles of the naphthalene cation-HCN and HCN-HCN interactions in determining the energetics and structures of the $C_{10}H_8^{++}(HCN)_n$ clusters, we calculated the binding energies of the lowest energy structures of the $C_{10}H_8^{++}(HCN)_n$ clusters (with respect to dissociation into $C_{10}H_8^{++}(HCN)_{n-1} + HCN$) using DFT at the M062X/6-311+G**, ω 97XD/6-311+G**, and the B3LYP/6-311++G** levels. The M06-2X and ω 97X-D functional are known to be accurate for van der Waals (vdW) and weak ion-molecule interactions.³⁹⁻⁴¹ We compare the results of the calculations of the $C_{10}H_8^{++}(HCN)_n$ clusters for $n = 1$ and 2 with the B3LYP functional using the 311++G**

basis set. Based on this comparison, we confirm the accuracy of the B3LYP functional for the calculations of larger clusters with $n = 3-6$.

All the M062X, ω 97XD and B3LYP functionals predict the lowest energy isomer of $C_8H_{10}^{+}(HCN)$ to be a bifurcated structure with HCN binding to two CH hydrogen atoms from the two condensed rings of the naphthalene cation by 2.44 Å (M062X and ω 97XD) and 2.50 Å (B3LYP) as shown in Figure 5-I (structure 1-a) and Figure 6 (structures 1-a). This geometry is similar to the calculated structures for the association of water with the benzene and naphthalene cations in the $C_6H_6^{+}(H_2O)$ and $C_8H_8^{+}(H_2O)$ clusters, respectively, and also for the association of HCN with the benzene cation.^{12,16,26} The binding energy of structure 1-a (Fig. 6) of the $C_8H_{10}^{+}(HCN)$ cluster calculated by the B3LYP function (7.8 kcal/mol corrected for ZPE) is in excellent agreement with the experimental ΔH° value (-7.1 kcal/mol) in contrast to the values calculated by the M06-2X and ω 97XD functions (9.1 and 8.8 kcal/mol, respectively) which appear to overestimate the binding energy. The other three low energy structures obtained using the M06-2X and ω 97XD functions are (1-b), (1-c) and (1-d) shown in Fig. 5-I. In (1-b) and (1-c) bifurcated structures are formed with two adjacent CH groups belonging to the same ring, while in structure (1-d) the HCN molecule lies above the plane of the naphthalene cation with the nitrogen atom pointing to plane of the cation. The binding energies of the four structures (1-a to 1-d, Fig. 5-I) range from 9.1 to 7.4 and 8.8 to 7.9 kcal/mol using the M06-2X and the ω 97XD functionals, respectively. The two functions give essentially the same low energy structures and the same binding energies. However, with the B3LYP function the calculated binding energy although smaller than the calculated values obtained using the M06-2X and the ω 97XD functionals, it is closer to the experimental ΔH° value.

Six low energy structures (2-a to 2-f) with binding energies ranging from 8.4 to 6.0 were identified for the $C_8H_{10}^{+}(HCN)_2$ cluster using the M06-2X and the ω 97XD functionals as shown in Fig. 5-II. The lowest energy isomer (2-a, Fig. 5-II) has the second HCN molecule forming another bifurcated structure with two CH hydrogen atoms from the two condensed rings of the naphthalene cation. The second lowest energy isomer of (structure 2-b, Fig. 5-II) shows the second HCN molecule hydrogen bonded to the first molecule. The very small difference in binding energy between structures (2-a) and (2-b)

indicates that HCN hydrogen bonding interaction with the $\text{CH}^{\delta+}$ group of the naphthalene cation ($\text{CH}^{\delta+}\cdots\text{N}$) is similar to the hydrogen bonding interaction with a second HCN molecule ($\text{NCH}\cdots\text{NCH}$).

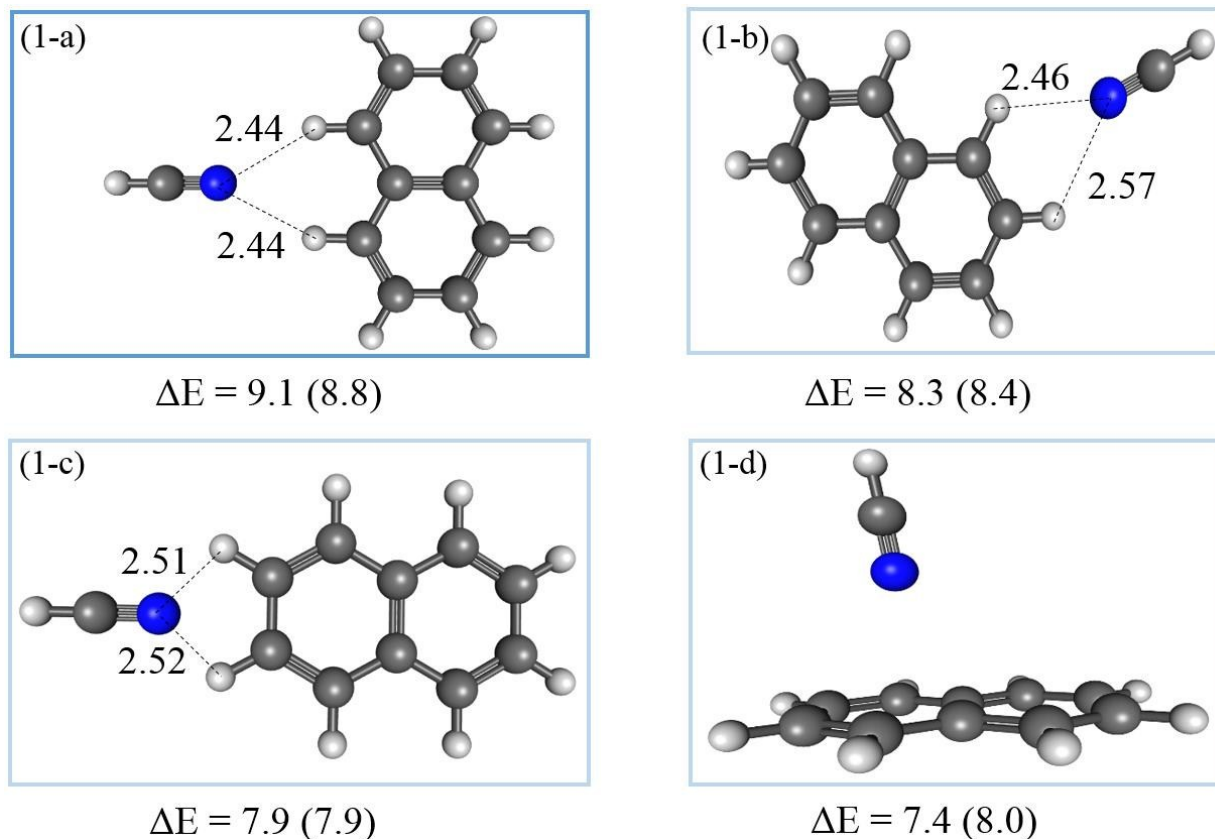


Figure 5-I. Structures of the four lowest energy isomers of the naphthalene⁺(HCN) complex obtained using the two functionals M062X and ω 97XD within the 6-311+G** basis set. The calculated binding energies ΔE in kcal/mol are given using the M062X and ω 97XD (in brackets) methods.

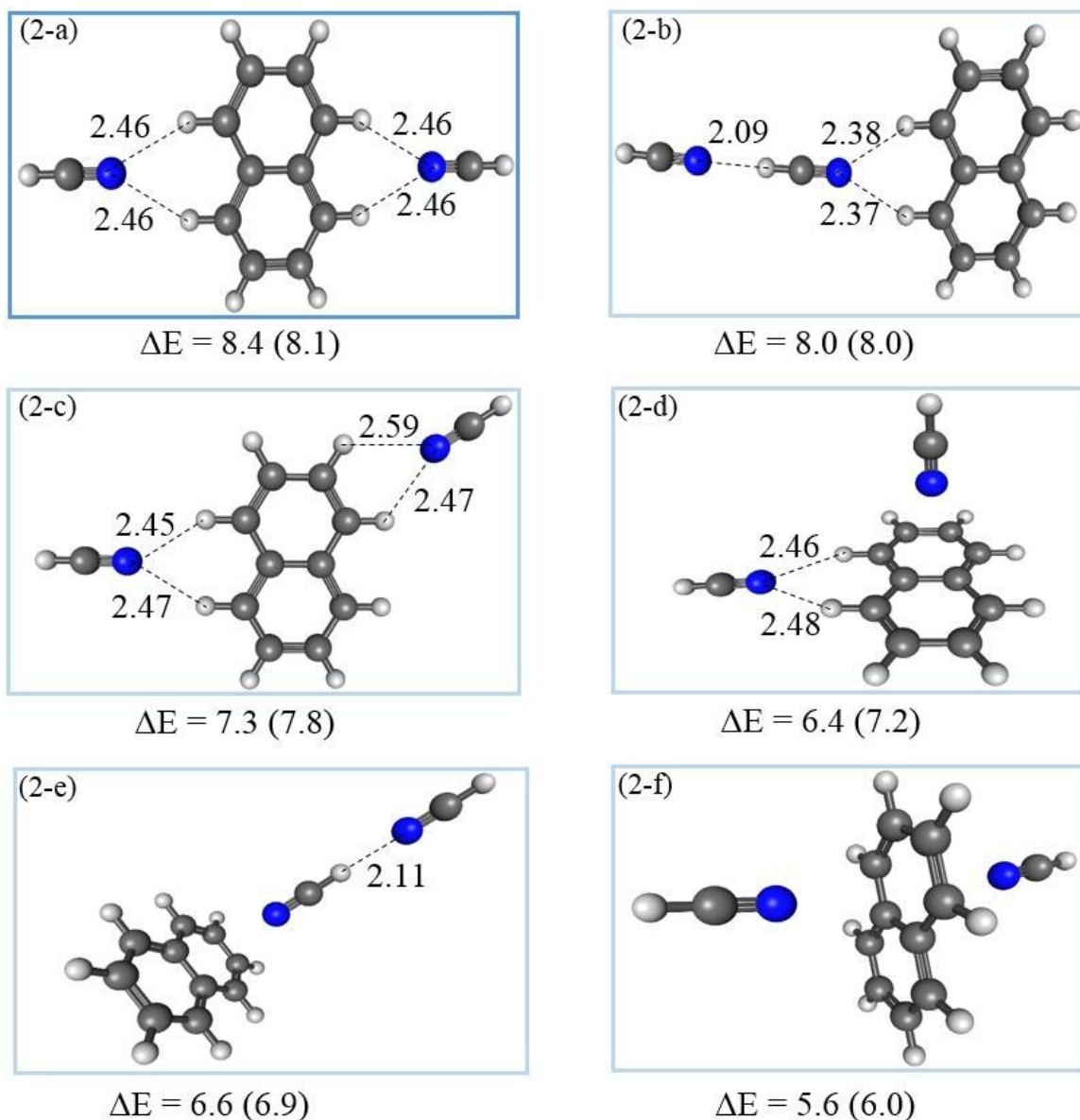


Figure 5-II. Structures of the six lowest energy isomers of the naphthalene⁺(HCN)₂ complex obtained using the two functionals M062X and ω 97XD within the 6-311+G** basis set. The calculated binding energies ΔE in kcal/mol are given using the M062X and the ω 97XD (in brackets) methods.

Based on the comparison between the M06-2X, the ω 97X-D and the B3LYP functionals, it can be concluded that these functions produce similar lowest energy structures of the $C_8H_{10}^{*+}(HCN)_n$ clusters although the M06-2X and the ω 97X-D functionals appear to overestimate the binding energies. Therefore, the B3LYP function at the 6-311++G(d,p) level was used to calculate the lowest energy structures of the $C_8H_{10}^{*+}(HCN)_n$ clusters with $n = 3$ and 4. The calculated structures and the corresponding binding energies are shown in Figure 6.

The lowest energy isomers of the $C_8H_{10}^{*+}(HCN)_n$ clusters with $n = 3$ and 4 show a tendency for the solvation of the naphthalene cation where two ($CH^{\delta+} \cdots N$) bifurcated hydrogen bonding sites with the ring hydrogen atoms on opposite sides of the naphthalene cation (structures 3-a and 4-a, Fig. 6). Isomer (3-b, Fig. 6) shows an extended hydrogen bonding chain with three HCN molecules attached to the naphthalene cation through a bifurcated structure. However, the formation of a longer hydrogen bonding chain with more than three HCN molecules on one side of the naphthalene cation may not be favorable as isomers (4-a) and (4-b) clearly preference for forming two bifurcated hydrogen bonding interactions along the opposite sides of the naphthalene cation.

The small energy differences between the different structures corresponding to the same cluster size imply that an ensemble of different configurations could exist at a given temperature and therefore, the measured binding energy represents an average value of the binding energies of these different structures. Furthermore, since the measured binding energies are obtained using equilibrium thermochemical measurements, it can be assumed that the different configurations are populated thermally.

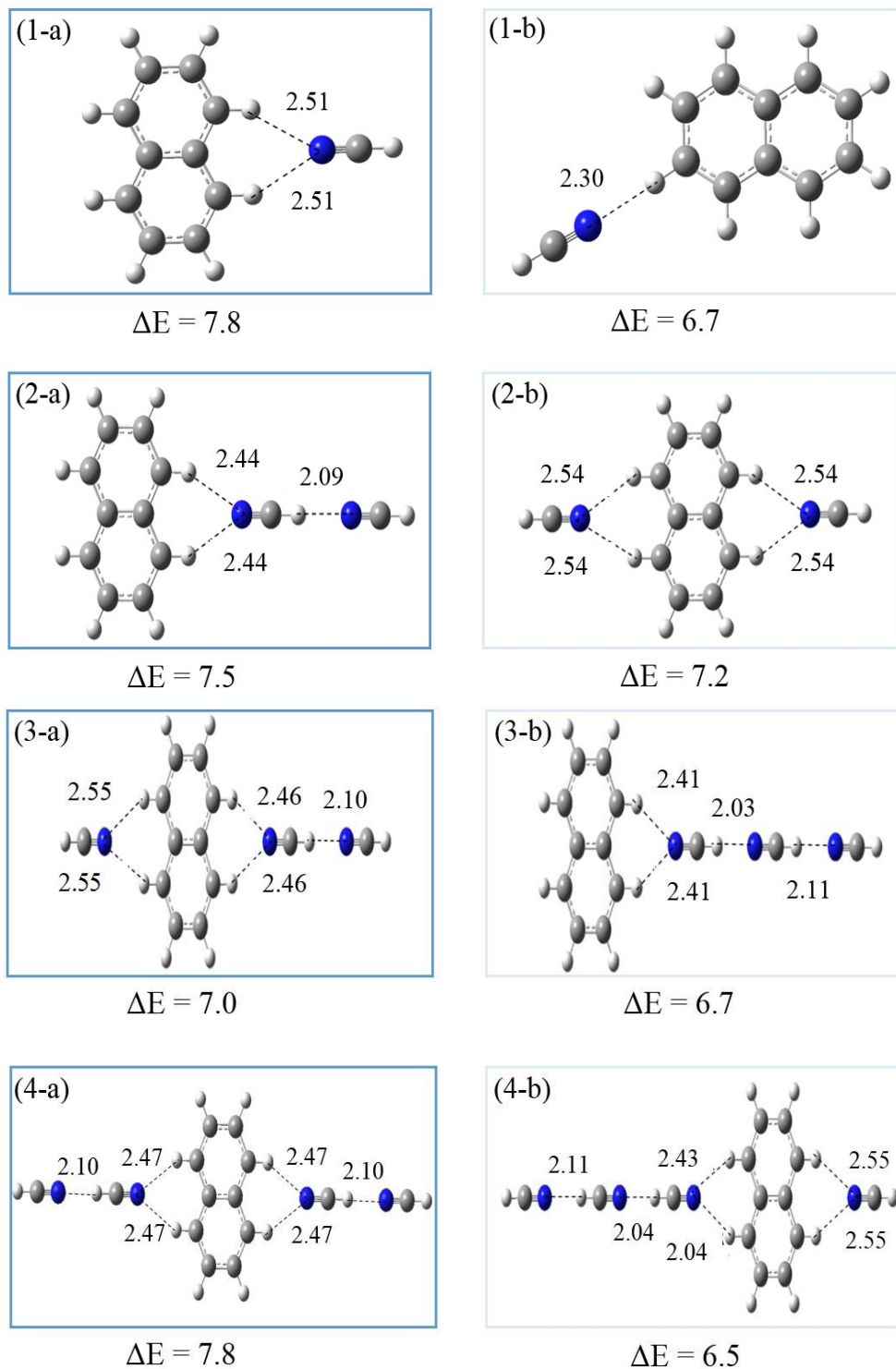


Figure 6. Structures of the two lowest energy isomers of the naphthalene⁺(HCN)_n clusters with n =1-4 obtained using the B3LYP method within the 6-311++G** basis set. The calculated binding energies ΔE are given in kcal/mol.

3.4 Structures of the Naphthalene⁺(CH₃CN)_n Clusters

Figure 7-I displays the optimized structures of the four lowest energy isomers of the C₈H₁₀⁺(CH₃CN) cluster calculated at the M06-2X/6-311++G** and ω97X-D/6-311++G** levels. The calculated binding energies range from 12.2 to 10.6 kcal/mol in good agreement with the experimental -ΔH° value of 11.3±1 kcal/mol. The lowest energy isomer (structure 1-a, Fig. 7-I) has a bifurcated structure with the nitrogen atom of acetonitrile interacting with two CH hydrogen atoms belonging to the two condensed rings of the naphthalene cation. The structure is similar to that of the lowest energy isomer of the C₈H₁₀⁺(HCN) cluster shown in Fig. 5-I. The other three isomers of the C₈H₁₀⁺(CH₃CN) cluster are also similar to those of the C₈H₁₀⁺(HCN) cluster thus confirming that these types of structures represent the most favorable interaction geometries between the nitrogen lone pair in HCN or CH₃CN molecule and the CH^{δ+} sites of the naphthalene cation.

The six lowest energy isomers of the C₈H₁₀⁺(CH₃CN)₂ cluster shown in **Figure 7-II** (structures 2-a to 2-f) have a broad range of binding energies (11.3 to 7.6 kcal/mol) representing three different types of structures where the two acetonitrile molecules form double bifurcated hydrogen bonding structures (2-a, 2-b and 2-c, Fig. 7-II), perpendicular and bifurcated structures (2-d and 2-e, Fig. 7-II) and a double perpendicular structure (2-f, Fig. 7-II). The symmetric double bifurcated hydrogen bonding structure (2-a, Fig. 7-II) is predicted to be the lowest energy structure, and both the M06-2X/6 and ω97X-d functions appear to overestimate the binding energy of this isomer (11.3 and 10.5 kcal/mol, respectively) as compared to the experimental -ΔH° value of 9.2±1 kcal/mol.

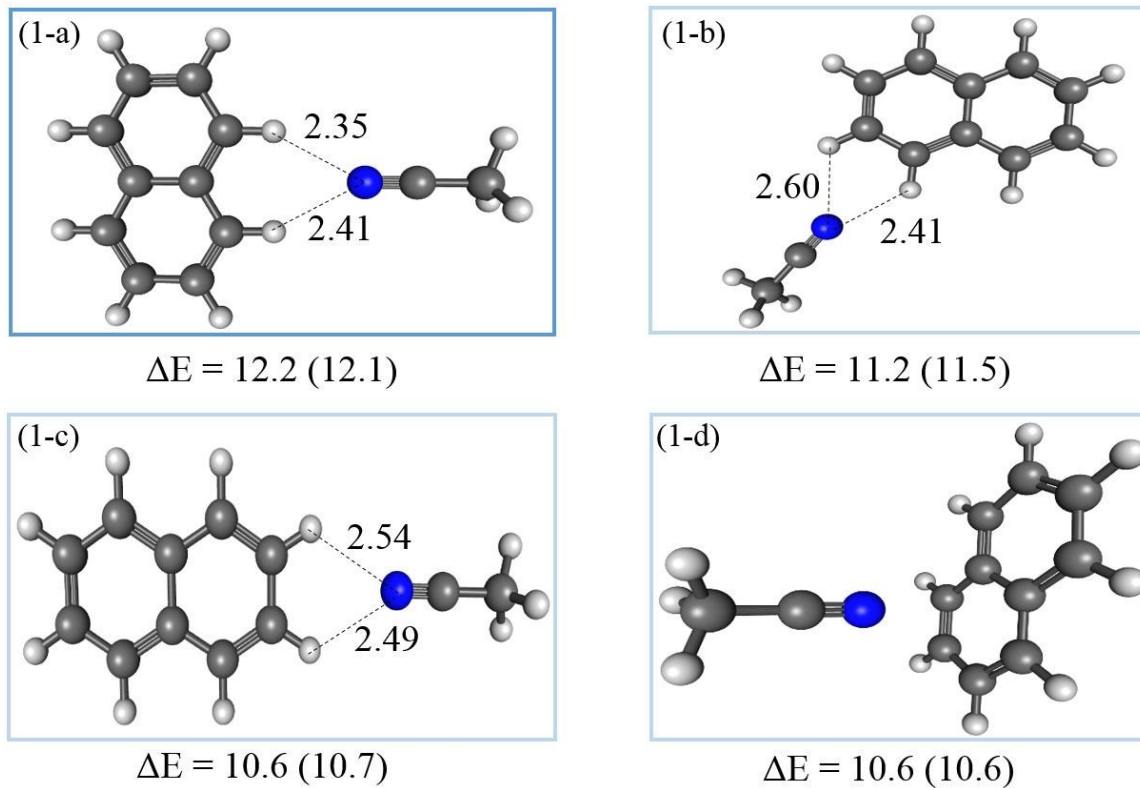


Figure 7-I. Structures of the four lowest energy isomers of the naphthalene⁺(CH₃CN) complex obtained using the two functionals M062X and ω 97XD within the 6-311+G** basis set. The calculated binding energies ΔE in kcal/mol are given using the M062X and ω 97XD (in brackets) methods.

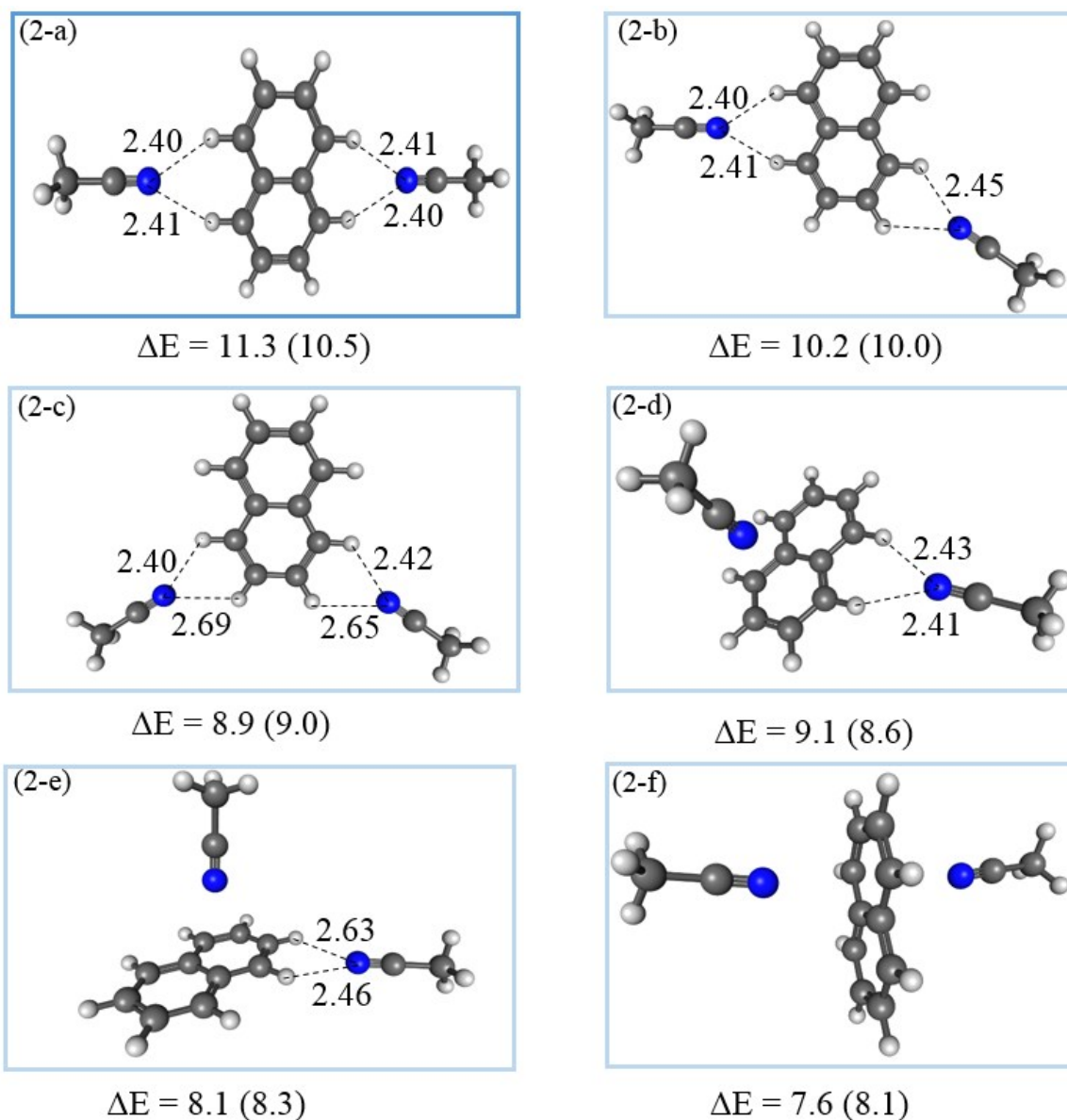


Figure 7-II. Structures of the six lowest energy isomers of the naphthalene⁺(CH₃CN)₂ complex obtained using the two functionals M062X and ω 97XD within the 6-311+G** basis set. The calculated binding energies ΔE in kcal/mol are given using the M062X and the ω 97XD (in brackets) methods.

The B3LYP function predicts the same lowest energy structures of the $C_8H_{10}^{*+}(CH_3CN)_{1,2}$ clusters as the M06-2X/6 and ω 97X-d functions as shown in **Figure 8**. However, the calculated binding energies with the B3LYP function of structures 1-a and 2-a (10.8 and 9.7 kcal/mol, respectively, Fig. 8) are in better agreement with the experimental $-\Delta H^\circ$ values of 11.3 ± 1 and 9.2 ± 1 kcal/mol, respectively than the values calculated using the M06-2X/6 and ω 97X-d functions (Figs 7-I and 7-II).

The lowest energy isomers of the $C_8H_{10}^{*+}(CH_3CN)_n$ clusters with $n = 3-6$ calculated at the B3LYP/6-311++G** level are also shown in Fig. 8. These structures build on the bifurcated hydrogen bonding structure motif which appears to be saturated for the naphthalene cation by the addition of four acetonitrile molecules as shown is isomer 4-a in Fig. 8. The calculated binding energies for the $C_8H_{10}^{*+}(CH_3CN)_{3,4}$ clusters (7.1 and 6.5 kcal/mol, respectively, Fig. 8) are in good agreement with the experimental $-\Delta H^\circ$ values of 7.2 ± 1 and 8.0 ± 1 kcal/mol, respectively.

The low energy structures of the $C_8H_{10}^{*+}(CH_3CN)_{5,6}$ clusters containing five and six acetonitrile molecules (structures 5-a and 6-a, Fig. 8) show evidence of saturation of the hydrogen bonding sites on the naphthalene cation by four acetonitrile molecules since the fifth and sixth molecules are calculated to attach to the coordinated acetonitrile molecules through weak $CH_3 \cdots N$ interaction ($CH^{\delta+} \cdots N \equiv C - CH_3 \cdots N \equiv C - CH_3$). Higher energy structures (5-b and 6-b, Fig.8) show the fifth and sixth acetonitrile molecules forming perpendicular structures through N...ring interactions above and below the plane of the naphthalene cation, respectively. The structures of the $C_8H_{10}^{*+}(CH_3CN)_{5,6}$ clusters represent the complete solvation of the naphthalene cation with acetonitrile molecules.

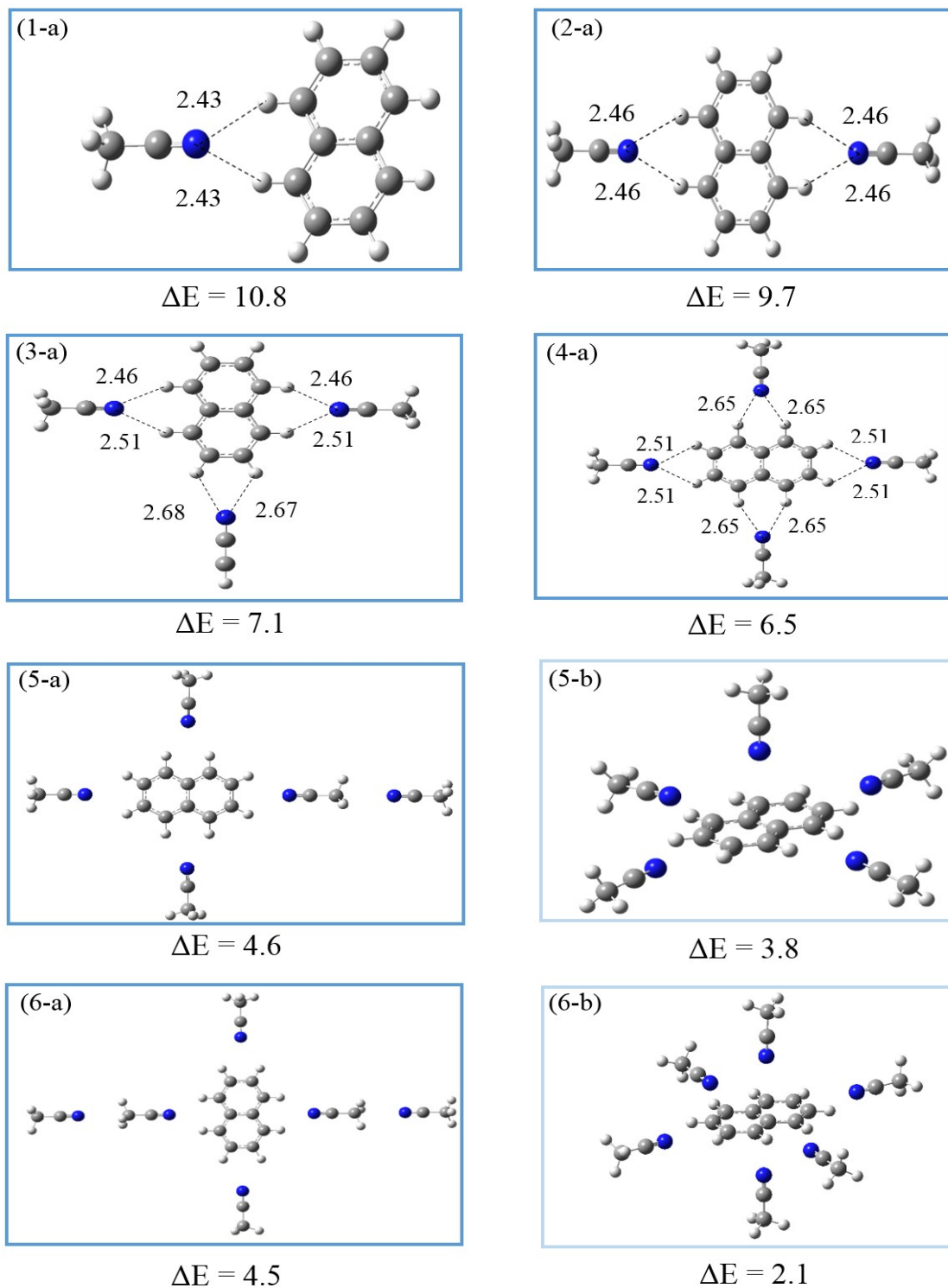


Figure 8. Structures of the lowest energy isomers of the naphthalene⁺(CH₃CN)_n clusters with n = 1-4, and the two lowest energy isomers with n = 5-6 obtained using the B3LYP method within the 6-311++G** basis set. The calculated binding energies ΔE are given in kcal/mol.

3.5. Comparison of the Interactions of Water, Methanol, Hydrogen Cyanide and Acetonitrile with the Naphthalene Radical Cation

It is of interest to compare the association behaviors of hydrogen cyanide and acetonitrile molecules towards the naphthalene cation with those involving water and methanol molecules. **Figure 9** compares the association enthalpies (ΔH°) and the lowest energy structures and binding energies calculated at the B3LYP/6-311++G** level for the $C_8H_{10}^{+\cdot}(H_2O)$,¹⁶ $C_8H_{10}^{+\cdot}(CH_3OH)$,¹⁶ $C_8H_{10}^{+\cdot}(HCN)$, and $C_8H_{10}^{+\cdot}(CH_3CN)$ clusters. The structures of the four clusters are similar and consist of unconventional bifurcated hydrogen bonding of the oxygen or nitrogen atom to two CH hydrogen atoms from the two condensed rings of the naphthalene cation.

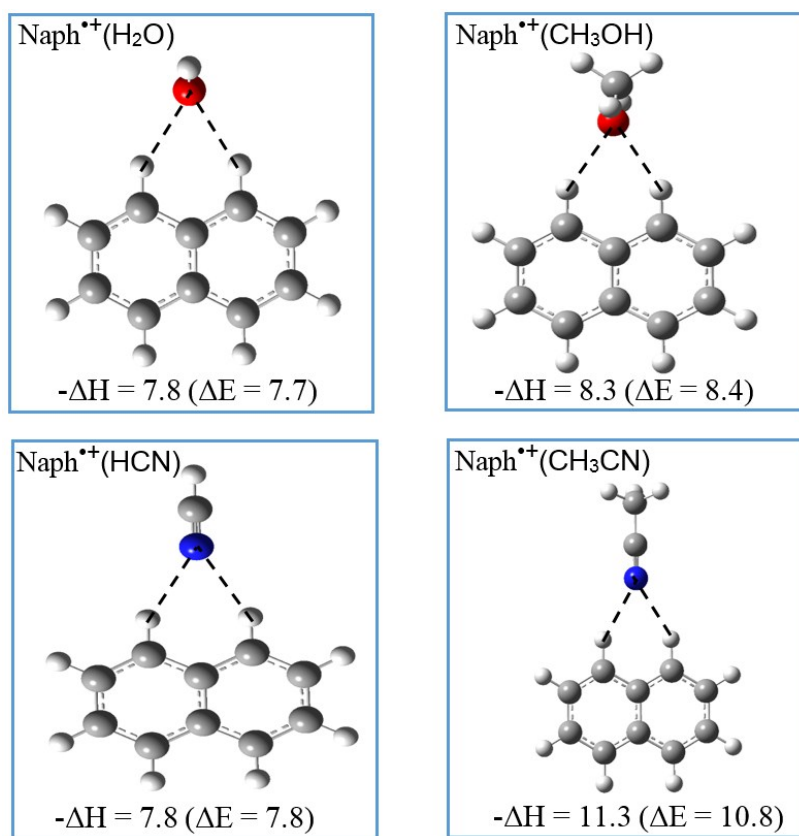


Figure 9. Lowest energy structures of the complexes of the naphthalene cation with H_2O ,¹⁶ CH_3OH ,¹⁶ HCN and CH_3CN with the calculated binding energies ΔE (kcal/mol) obtained using the B3LYP method within the 6-311++G** basis set. The experimental ΔH° (kcal/mol) is shown for comparison with the calculated ΔE .

The association enthalpies ΔH° for water (7.8 ± 1), methanol (8.3 ± 1) and HCN (7.1 ± 1) are nearly similar, and smaller than that of acetonitrile (11.3 ± 1). This is mostly due to stronger ion dipole interaction in the $C_8H_{10}^{+}(CH_3CN)$ cluster given that the dipole moment of acetonitrile, HCN and water are 3.92, 2.98 and 1.85 Debye, respectively.³¹

Figure 10 compares the experimental sequential enthalpy of association ($-\Delta H^\circ_{1,n}$) of HCN and acetonitrile molecules to different organic cations. As shown in Fig. 10-a, HCN binds to the phenylacetylene (10.5 kcal/mol)²⁸ and to the benzene (9.2 kcal/mol)²⁶ radical cations more strongly than it binds to the naphthalene radical cation (7.1 kcal/mol).

For the phenylacetylene⁺(HCN) complex, the lowest energy isomer shows the N-atom of the HCN molecule interacting with the acetylenic CH by a 2.0 \AA conventional hydrogen bond.²⁸ This indicates that the conventional $C-H^{\delta+} \cdots N$ hydrogen bond is stronger than the unconventional bifurcated hydrogen bonding of the nitrogen atom to two CH hydrogen atoms from the ionized ring in the benzene or the naphthalene cation. The interaction is weaker with the naphthalene cation as compared to the benzene cation due to the charge delocalization on the larger naphthalene cation and therefore, the effective partial charges on the ring CH hydrogen atoms are smaller in the naphthalene cation as compared to the benzene cation. The effect of charge delocalization on the organic ion is clearly observed by comparing the binding energies of $c\text{-}C_3H_3^+(CH_3CN)_n$, benzene⁺(CH_3CN)_n and naphthalene⁺(CH_3CN)_n clusters shown in Fig. 10-b. The naphthalene⁺(CH_3CN)_n clusters show the weakest sequential binding energies among the ions shown in Fig. 10-b. This is again a result of charge delocalization on the naphthalene radical cation which leads to weaker charge-dipole interactions in comparison with the $c\text{-}C_3H_3^+(CH_3CN)_n$ clusters.¹³

It is interesting to note that in both the $C_{10}H_8^+(HCN)_n$ and $C_{10}H_8^+(CH_3CN)_n$ clusters, the sequential binding energy decreases stepwise to about 6-7 kcal/mol by three HCN or CH_3CN molecules, approaching the macroscopic enthalpy of vaporization of liquid HCN (6.0 kcal/mol) or liquid acetonitrile (7.9 kcal/mol).³¹ This limit is reached in the $C_6H_6^+(CH_3CN)_n$ clusters with four CH_3CN molecules but for the $C_3H_3^+(CH_3CN)_n$ clusters, the sequential binding energy for the third acetonitrile molecule (12.0

kcal/mol)¹³ is still significantly higher than the enthalpy of vaporization of liquid acetonitrile.

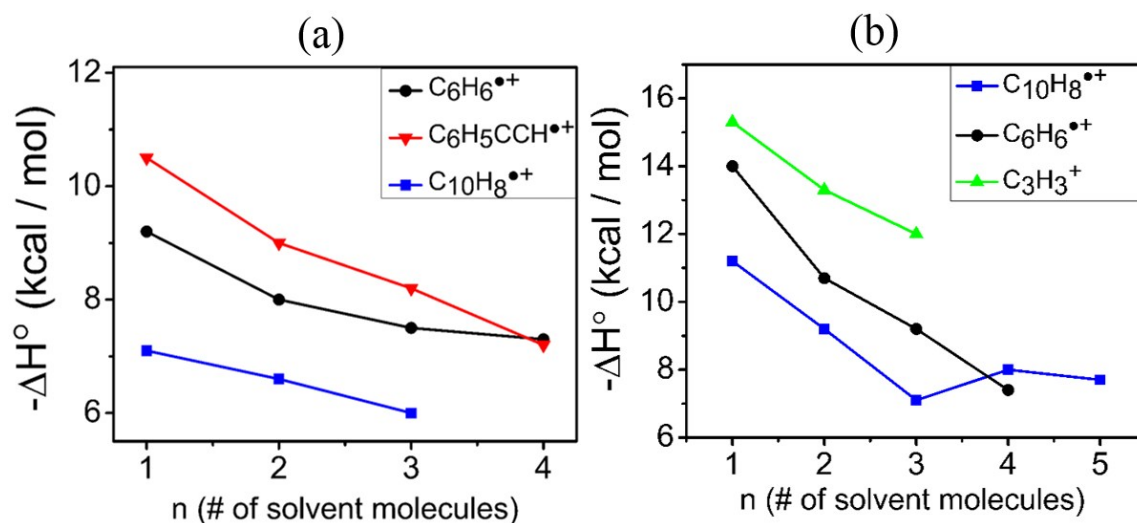


Figure 10. (a) Experimental sequential enthalpy of association ($-\Delta H^\circ_{n-1,n}$) of HCN molecules to the benzene²⁶ ($C_6H_6^{\bullet+}$), phenylacetylene²⁸ ($C_6H_5CCH^{\bullet+}$) and naphthalene ($C_{10}H_8^{\bullet+}$) radical cations (Estimated errors in $\Delta H^\circ \pm 1$ kcal/mol).

Figure 10. (b) Experimental sequential enthalpy of association ($-\Delta H^\circ_{n-1,n}$) of acetonitrile molecules to the *c*-C₃H₃ cation¹³ ($C_3H_3^+$) and to the benzene²⁶ ($C_6H_6^{\bullet+}$) and naphthalene ($C_{10}H_8^{\bullet+}$) radical cations (Estimated errors in $\Delta H^\circ \pm 1$ kcal/mol).

4. Summary and Conclusions

Equilibrium thermochemical measurements using a mass-selected ion mobility drift cell technique have been utilized to investigate the binding energies and entropy changes associated with the stepwise association of HCN and CH₃CN molecules with the naphthalene radical cation in the $C_8H_{10}^{\bullet+}(HCN)_n$ and $C_8H_{10}^{\bullet+}(CH_3CN)_n$ clusters with $n = 1-3$ and $1-5$, respectively. The binding energy of CH₃CN to the naphthalene cation (11.3 kcal/mol) is much stronger than that of HCN (7.1 kcal/mol) mostly due to a stronger ion-dipole interaction attributed to the large dipole moment of acetonitrile (3.9 D). The lowest energy structures of the $C_{10}H_8^{\bullet+}(HCN)_n$ and $C_{10}H_8^{\bullet+}(CH_3CN)_n$ clusters indicate that

the first HCN or CH₃CN molecule forms unconventional bifurcated hydrogen bonds with two CH hydrogen atoms from the two condensed rings of the naphthalene cation. Further HCN molecules can form both unconventional hydrogen bonds with the hydrogen atoms of the naphthalene cation (CH^{δ+}...NCH), and conventional linear hydrogen bonding chains involving HCN...HCN interactions among the associated HCN molecules. HCN molecules tend to form “externally solvated” structures with the naphthalene cation where the naphthalene ion is hydrogen bonded to the exterior of an HCN...HCN chain. For the C₁₀H₈⁺(CH₃CN)_n clusters, “internally solvated” structures are favored where the acetonitrile molecules are directly interacting with the naphthalene cation through CH^{δ+}...N unconventional ionic hydrogen bonds. In both the C₁₀H₈⁺(HCN)_n and C₁₀H₈⁺(CH₃CN)_n clusters, the sequential binding energy decreases stepwise to about 6-7 kcal/mol by three HCN or CH₃CN molecules, approaching the macroscopic enthalpy of vaporization of liquid HCN (6.0 kcal/mol).

ACKNOWLEDGMENT

We thank the National Science Foundation (CHE-1463989) for the support of this work.

References

1. M. Meot-Ner (Mautner), *Chem. Rev.* **2012**, *112*, PR22-103; “The Ionic Hydrogen Bond”, *Chem. Rev.* **2005**, *105*, 213-284.
2. S. Scheiner, (Editor), *Noncovalent Forces*, Springer International Publishing, Switzerland, 2015.
3. P. Hobza; D. K. Muller, *Non-covalent Interactions*, Royal Society of Chemistry, Cambridge, U. K., 2009.
4. S. Tsuzuki, In *Intermolecular Forces and Clusters I*; Wales, D. J., Ed.; Springer Berlin Heidelberg: 2005; Vol. 115, p 149.
5. B. E. Conway, *Ionic Hydration in Chemistry and Biophysics*, Elsevier, Amsterdam, New York, 1981.
6. C. Tanford, *The Hydrophobic Effect: Formation of Micelles and Biological Membranes*; 2d ed.; Wiley: New York, 1980.
7. M. Nuevo; S. N. Milam; S. A. Sandford; J. Elsila; J. P. Dworkin, *J. P. Astrobiology* **2009**, *9*, 683-695.

8. C. Menor-Salvan; M. R. Marin-Yaseli, *Chem. Soc. Rev.* **2012**, 41, 5404-5415.
9. R. S. Gudipati, R. S.; L, J, Allamandola, *Astrophys. J.* **2006**, 638, 286–292.
10. Y. M. Rhee; T. J. Lee, M. S. Gudipati; L. J. Allamandola; M. Head-Gordon, *Proceedings of the National Academy of Sciences USA* **2007**, 104, 5274-5278.
11. Y. Ibrahim; E. Alsharaeh; K. Dias; M. Meot-Ner; M. S. El-Shall, *J. Am. Chem. Soc.*, **2004**, 127, 12766-12767.
12. Y. Ibrahim; E. Alsharaeh; M. Meot-Ner; M. S. El-Shall; S. Scheiner, *J. Am. Chem. Soc.* **2005**, 127, 7053-7064.
13. R. Mabrouki; Y. Ibrahim; E. Xie; M. Meot-Ner; M. S. El-Shall, *J. Phys. Chem. A.* **2006**, 110, 7334-7344.
14. P. O. Momoh; M. S. El-Shall, *Phys. Chem. Chem. Phys.* **2008**, 10, 4827-4834.
15. P. O. Momoh; A. M. Hamid; S. A. Abrash; M. S. El-Shall, *J. Chem. Phys.* **2011**, 134, 204315.
16. I. K. Attah; S. P. Platt; M. Meot-Ner; S. G. Aziz; A. O. Alyoubi; M. S. El-Shall, *Chem. Phys. Letters* **2014**, 613, 45-53.
17. Y. Ibrahim; R. Mabrouki; M. Meot-Ner: M. S. El-Shall, *J. Phys. Chem. A.* **2007**, 111, 1006-1014.
18. A. M. Hamid; P. Sharma; R. Hilal; S. Elroby; S. G. Aziz; A. O. Alyoubi; M. S. El-Shall, *J. Chem. Phys.* **2013**, 139, 084304.
19. Q. B. Li; D. J. Jacob; R. M. Yantosca; C. L. Heald; H. B. Singh; M. Koike; Y. J. Zho; G. W. Sachse; D. G. Streets, *J. Geophys. Atmos.* **2003**, 108, 8827.
20. E. Herbst; E. F. van Dishoeck, *Annul. Rev. Astron. Astrophys.* **2009**, 47, 427-480.
21. C. N. Matthews; R. A. Ludicky, *Adv. Space Res.* **1992**, 12, 21-32.
22. M. J. Mumma; M. A. DiSanti; K. Magee-Sauer; B. P. Bonev; G. L. Villanueva; H. Kawakita; N. D. Russo; E. L. Gibb; G. A. Blake; J. E. Lyke; R. D. Campbell; J. Aycock; A. Conrad; G. M. Hill, *Science*, **2005**, 310, 270.
23. F. Lahuis; E. F. van Dishoeck; A. C. A. Boogert; K. M. Pontopiddan; G. A. Blake; C. P. Dullemond; N. J. Evans II; M. R. Hogerheijde; J. K. Jørgensen; J. E. Kessler-Silacci; C. Knez, *Astrophys. J. Lett.*, **2006**, 636, L145.
24. C. N. Matthews; R. D. Minard, R. D. *Faraday Discuss.* **2006**, 133, 393-401.
25. S. Pizzarello; W. Holmes, *Geochim. Cosmochim. Acta* **2009**, 73, 2150-2162.
26. A. M. Hamid; A. R. Soliman; M. S. El-Shall, *J. Phys. Chem. A* **2013**, 117, 1069-1078.
27. I. K. Attah; A. M. Hamid; M. Meot-Ner; S. G. Aziz; A. O. Alyoubi; M. S. El-Shall, *J. Phys. Chem. A* **2013**, 117, 10588-10579.

28. A. M. Hamid; A. R. Soliman; M. S. El-Shall, *Chem. Phys. Letters* **2012**, **543**, 23-27.
29. A. M. Hamid; M. S. El-Shall; R. Hilal; S. Elroby; S. G. Aziz, *J. Chem. Phys.* **2014**, 141, 054305.
30. M. Meot-Ner; C. V. Speller, *J. Phys. Chem.* **1989**, 93, 3663-3666.
31. NIST Chemistry Web Book, *NIST Standard Reference Database Number 69; National Institute of Standards and Technology: Gaithersburg MD, 20899* (<http://webbook.nist.gov>).
32. Y. Zhao; D. G. Truhlar, *Theor. Chem. Acc.* **2008**, 120 (2008) 215-241.
33. J.-D. Chai; M. Head-Gordon, *Phys. Chem. Chem. Phys.* **2008**, 10, 6615-6620.
34. (a) A. D. McLean; G. S. Chandler, *J. Chem. Phys.* **1980**, 72, 5639-5648. (b) K. A. Peterson; D. E. Woon; T. H. Dunning Jr., *J. Chem. Phys.* **1994**, 100, 7410-7415.
35. M. J. Frisch; G. W. Trucks; H. B. Schlegel; G. E. Scuseria; M. A. Robb; J. R. Cheeseman; G. Scalmani; V. Barone; B. Mennucci; G. A. Petersson *et al.* *Gaussian 09, revision A.1*, Gaussian, Inc., Wallingford CT, **2009**.
36. C. A. Deakyne; M. Meot-Ner; C. L. Campbell; M. G. Hughes; S. P. Murphy, *J. Chem. Phys.* **1986**, 90, 4648.
37. G. M. Daly; J. Gao; M. S. El-Shall, *Chem. Phys. Letters* **1993**, 206, 500-508.
38. D. S. Venables; C. A. Schmuttenmaer, *J. Chem. Phys.* **1998**, 108, 4935.
39. Zhao, Y.; Truhlar, D. G. *Acct. Chem. Res.* **2008**, **41**, 157-167.
40. Tsuzuki, S.; Fujii, A. *J. Phys. Chem. Chem. Phys.* **2008**, 10, 2584-2594.
41. I. K. Attah; S. P. Platt; M. Meot-Ner; M. S. El-Shall; R. Peverati; M. Head-Gordon, *J. Phys. Chem. Lett.* **2015**, 6, 1111-1118.